Available online at www.sciencedirect.com
SCIENCE DIRECT®
Journal of Chromatography A, 1093 (2005) 156–166
JOURNAL OF CHROMATOGRAPHY A
www.elsevier.com/locate/chroma

Natural sample fractionation by FlFFF–MALLS–TEM: Sample stabilization, preparation, pre-concentration and fractionation

M. Baalousha[a,*], F.V.D. Kammer[b], M. Motelica-Heino[c], P. Le Coustumer[a]

[a] *Center of Development of Applied Geology, University of Bordeaux 1, Bat B18, Avenue des Facultés, 33400 Talence, France*
[b] *Department of Geological Science, Environmental Geology, Vienna University, 1090 Wien, Austria*
[c] *BRGM, Avenue Claude Guillemin, 45060 Orléans, France*

Received 1 June 2005; received in revised form 21 July 2005; accepted 25 July 2005
Available online 16 August 2005

Abstract

Two flow field flow fractionation (FlFFF) systems: symmetrical (SFlFFF) and asymmetrical (ASFlFFF) were evaluated to fractionate river colloids. Samples stability during storage and colloids concentration are the main challenges limiting their fractionation and characterization by FlFFF. A pre-fractionation (<0.45 μm) and addition of a bactericide such as NaN_3 into river colloidal samples allowed obtaining stable samples without inducing any modification to their size. Stirred cell ultra-filtration allowed colloidal concentration enrichment of 25-folds. Scanning electron microscope (SEM) micrographs confirmed the gentle pre-concentration of river samples using the ultra-filtration stirred cell. Additionally, larger sample injection volume in the case of SFlFFF and on channel concentration in the case of ASFlFFF were applied to minimize the required pre-concentration. Multi angle laser light scattering (MALLS), and transmission electron microscope (TEM) techniques are used to evaluate FlFFF fractionation behavior and the possible artifacts during fractionation process. This study demonstrates that, FlFFF–MALLS–TEM coupling is a valuable method to fractionate and characterize colloids. Results prove an ideal fractionation behavior in case of Brugeilles sample and steric effect influencing the elution mode in case of Cézerat and Chatillon. Furthermore, comparison of SFlFFF and ASFlFFF fractograms for the same sample shows small differences in particle size distributions.

Keywords: FlFFF; MALLS; TEM; SEM; River colloids; Pre-concentration; Steric elution

1. Introduction

Many physicochemical processes taking place in natural aquatic systems such as: colloids settling, re-suspension, adsorption, and transport depend on their size distribution [1,2]. Different components of colloidal matter (i.e. humic substances, iron oxides, alumiosilicates, etc.) often occur in a characteristic size range, which may result in differential transport, deposition, or pollutant adsorption [3–8]. Thus, colloidal size fractionation and determination are indispensable, which implies the necessity for a high-performance fractionation technique and sensible detection systems. Flow field flow fractionation (FlFFF) was proved to be a valuable technique for colloidal matter fractionation [9,10]. However, several factors such as: sample stability during storage time and the low concentration of rivers colloids, often 1–100 mg l^{-1}, combine to make the characterization of rivers colloids extremely difficult [11,12].

A stable colloidal sample is a sample resistant to aggregation and removal by settling, or filtration. In order to optimize sample stability, minimize artifacts, minimize chemical, or physical modifications induced during sampling and storage time; Buffle and Leeuwen [12,13] suggested that: (i) all measurements (including fractionation and colloid structure studies) must be carried out within 2–3 days after sampling since significant changes by coagulation or bacterial activity mainly occur after this period, provided storage is done at 4 °C in the dark, (ii) physical and chemical changes of samples must be minimized, (iii) sampling vessels must be pre-equilibrated, and (iv) several techniques must be used in parallel, both to derive as much structural information as pos-

* Corresponding author. Tel.: +33 540008798; fax: +33 556807138.
E-mail address: mbalousha@yahoo.co.uk (M. Baalousha).

0021-9673/$ – see front matter © 2005 Elsevier B.V. All rights reserved.
doi:10.1016/j.chroma.2005.07.103

sible and to act as cross check on the possible artifacts, which may occur during sample preparation and analysis.

The typical low concentration of colloidal river matter can be overcome applying pre-concentration process prior to analysis. A pre-concentration of 1:10 to 1:1000 is then required before fractionation by FlFFF [14,15]. Several methods are available for colloidal sample concentration including ultra-filtration, centrifugation, coagulation, and on channel concentration [14,16]. The pre-concentration step is time consuming process and is a potential cause of sample aggregation and losses. Consequently, reducing the required degree of concentration would be a significant advance [11].

FlFFF has been used extensively in biological and polymers research, but it was much less used in environmental research. This is presumably due to the low stability and concentration of natural samples [17]. To date, two environmental applications of the FlFFF have been explored. The first is the characterization of river-borne colloids [2,11,16] and soil colloids [15]. The second is the determination of molecular weight distribution and size of humic substances [9,18,19].

The rigors of FlFFF theory has been extensively described elsewhere [9,17,20], and need not concern us here. FlFFF theory uses the Stokes formula for converting diffusion coefficient into particle size. Consequently, the size and size-distributions determined from FlFFF system differ from the theoretical values as soon as colloids deviate from homogeneous hard spheres and only an equivalent diameter is retrieved. Interferences inside the FlFFF channel such as: overload effects, steric/hyperlayer elution mode transition (i.e. elution of large and small particles at the same elution volume), particle-wall interactions, and shape selective retention are frequently observed for natural samples. These interferences may hamper the interpretation of FlFFF fractograms and limit its environmental applications. Therefore, FlFFF needs to be coupled to sensitive independent size measuring techniques such as spectroscopic or imaging techniques [10].

UV–vis spectrophotometers have long been used for the determination of the relative amount of mass in the separated fractions, simply assuming that absorbance, or turbidity is proportional to the mass concentration [10]. One possible uncertainty using the UV–vis detector arises from the underestimation of small particles size concentration (less than the radiation wavelength 254 nm) and the dependence of the signal on particle and other parameters [2]. Fluorescence detection (FLD) has also been used as a concentration detector in nephelometric mode as a simple light scattering detector [21]. Multi-angle laser light scattering (MALLS) is a powerful technique, permitting the determination of particles size by measuring scattered light intensity at a range of fixed angles. The light scattering theory has been extensively described in [22,23]. The main advantage of the MALLS technique lies in that, it is an absolute technique and FlFFF independent. Direct examination of colloidal particles by transmission electron microscope (TEM) is very useful as it provides an independent determination of particle size [14], which may then be used to verify the elution mode of particles and to determine their thickness, aspect ratio [24], geometric surface area [10], and qualitative elemental composition when coupled with energy dispersive X-ray spectroscopy (EDS) [10,16]. The FlFFF–MALLS–TEM coupling allows 3D calculation of colloids dimensions, i.e. thickness, aspect ration, and surface area [24,25].

Colloidal size determination suffers many limitations including: the limited size range covered, inaccuracies in theories, lack of resolution, and inability to fractionate and size samples. These deficiencies in the commonly used separation methods have hindered attempts to gain information on colloidal size distribution. This work aims to provide a sample processing strategy from sampling to fractionation process, which should account for: (i) stability of natural (river) colloids, (ii) concentration, separation, and size determination of river colloidal samples by FlFFF–UV-FLD–MALLS–TEM, and (iii) elucidate the different possible behaviors of natural colloidal samples during the fractionation process and how the MALLS and TEM can be used to discover these behaviors.

2. Materials and methods

2.1. Sampling and sampling locations

First, one sample was collected from the Loire river at Orleans to test its stability under storage conditions. The stability test will be described in Section 2.3. Then eight other samples were collected from the Loire River watershed. The Loire River watershed, sampling sites, and sample collection is extensively described in Baalousha et al. [26]. Briefly, the Loire River from its source in the Massif Central to the Atlantic Ocean, is 1010 km long. The total basin area is 117,800 km^2. The Loire is one of the principal European riverine inputs of water to the Atlantic Ocean. The Loire watershed is characterized by varied geological formations. The bedrock composition of the studied area comprises (i) older plutonic rocks granite, gneiss, and mica schist (500–300 My), and a large volcanic area, as wall as (ii) a sedimentary bedrock the (Paris Basin) consists primarily of sedimentary deposits (200–6 My).

2.2. Instruments

Two FlFFF systems have been used in this study: symmetrical (SFlFFF) and asymmetrical (ASFlFFF). The SFlFFF system used is F1000 model Universal FFFractionator (Postnova Analytics Europe, Landsberg, Germany). The channel dimensions are: 29 cm length, 2.5 cm width, and 254 μm thickness. A 10 kD regenerated cellulose membrane (Postnova Analytics Europe, Landsberg, Germany) was used as the accumulation wall. ‘Milli-Q’ water (Millipore, Bedford,

UK) with 0.025% sodium dodecysulfonate and 0.02% NaN_3 in composition was used as a carrier solution. The cross flow was maintained with a Pharmacia P500 double piston pump and the carrier solution was delivered by a Hewlett-Packard HP1100 isocratic HPLC pump. The SFlFFF separation conditions were: 1 ml min^{-1} channel flow and 0.3 ml min^{-1} cross flow. The ASFlFFF system was purchased from by Wyatt Technology Corp. (Santa Barbara, CA, USA). The accumulation wall of the channel is made of an ultra-filtration membrane of regenerated cellulose with 1 kD cut-off (Postnova Analytics, Europe, Landsberg, Germany). A spacer of 490 μm height delimits the channel thickness. A solution of 0.02% sodium dodecysulfonate (SDS) in ultra-pure water was used as a carrier solution. The carrier solution was degassed prior to use by a 1100 Series vacuum degassed model G1379A and then delivered to the channel by mean of a 1100 HPLC Iso-pump model G1310A from Hewlett-Packard Europe. The ASFlFFF channel was controlled by the Eclipse separation system available from Wyatt Technology Corp. (Santa Barbara, CA, USA). The ASFlFFF separation conditions were: injection and focusing time of 11 min, injection flow rate 0.2 ml min^{-1}, focusing time of 1 min, channel flow 1.0 ml min^{-1}, and gradient cross flow starting at 0.25 ml min^{-1} and decreasing linearly to 0.1 ml min^{-1} during 50 min.

Nanospherical polystyrene polymers standards particles (Duke Scientific, Palo Alto, CA) of sizes 50 ± 2, 73 ± 2.6, 102 ± 3, 150 ± 4, 220 ± 6, 343 ± 9, 494 ± 4 nm hydrodynamic diameter were used for SFlFFF calibration and ASFlFFF as previously described in [11,15,24,25]. The hydrodynamic radius (R_h) was correlated to the elution volume (V_e) of the SFlFFF and ASFlFFF respectively, by Eqs. (1) and (2) with a regression coefficient $R^2 = 0.99$. Eq. (2) shows a parabolic equation due to the decrease of cross flow with elution time. R_h is the hydrodynamic radius and V_e is the elution volume.

$$R_h = 9.1466 V_e \quad (1)$$

$$R_h = 0.0339 V_e^2 + 5.5106 V_e - 1.0056 \quad (2)$$

Concentration measurements were performed with an HP1100 Hewlett Packard UltraViolet-Diode Array Detector (UV-DAD) and a Fluorescence Detector (FLD). The UV-DAD was operated at a wavelength of 250 nm. The FLD was operated at 320 nm excitation and emission wavelength and used as concentration detector in scattering (nephlometric) mode [21]. The detailed methodology to use the FLD to calculate the differential weight fraction corresponding to each R_g (RMS radius, or radius of gyration, R_g) is described in details elsewhere [25].

The MALLS is an 18 angles DAWN Enhanced Optical System (DAWN EOS) from (Wyatt Technology Corp., Santa Barbara, CA, USA). It utilizes a laser source at a wavelength of 690 nm. The scattered light is measured simultaneously at 16 different angles (typically 15–160°, two angles are not usable with flow cell and aqueous carrier solution). FlFFF

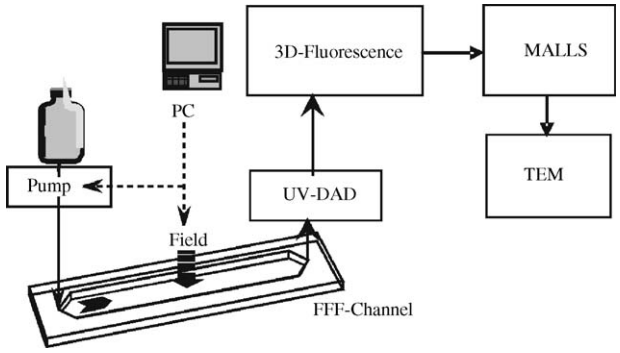

Fig. 1. Schematic representation of the FFF channel and the coupled detectors (FFF-UV-FLD–MALLS–TEM).

was coupled to the different detectors (UV-FLD–MALLS, and TEM) as shown in Fig. 1.

Wyatt Technology Corp. (Santa Barbara, CA, USA) ASTRA 4.73 program was used to collect signals from the UV, FLD, and MALLS detectors, and to process data to calculate R_g and its distribution. To calculate R_g from the angular distribution of the excess Rayleigh ratio, the linear ZIMM fitting method was used. This method is to date the most successful for natural colloids, and hence, irregular shaped colloids [21,25].

The photon correlation spectroscopy (PCS) is a Zetasizer Nano series model ZEN3600 (Malvern Instruments GmbH, Herrenberg, Germany) operating at a wavelength of 690 nm. It was used to determine the mean size (in the range from 0.6 to 6 μm) of colloids for the sample collected from the Loire at Orleans site. This technique is based on the theory of Dynamic Light Scattering (DLS) measurements. DLS/PCS uses a laser beam to probe a small volume of a suspension of particles and measures the fluctuation in the intensity of the scattered light, which is related to the Brownian motion, and therefore, to the particle size. Physical principles and mathematical treatment of the PCS data (converting autocorrelation functions to distribution functions, or average characteristics) are detailed elsewhere [27,28]. The detection limit, the effect of polydispersity of samples, and the refractive index value obtained with synthetic colloids using the PCS are also studied in details by Gun'ko et al. [27]. An aliquot of 4 ml of each sample was used to measure average colloidal size at different times after sampling.

Both TEM and SEM were used to image colloids and control their size distribution. A Phillips CM10 TEM (Eindhoven, The Netherlands) with a LaB_6 filament at emission 3 (from a selection of one to six) and an accelerating voltage of 100 keV was used to minimise the reaction of the sample under the electron beam. The aperture of the second condenser lens was nominally 50 μm and the spot size of the electron beam was 1 μm nominative to get the best compromise between illumination and potential degradation of the sample. Contrasted Bright Field (CBF) modes were used for textural analysis. An aliquot (1 ml) was collected from the FlFFF eluate each 4 min for TEM analysis. TEM samples

were prepared as follow: a droplet of sample solution was deposited over a TEM grid which was then dried by adsorbing the water by a filter paper. TEM grids are 300 mesh Cu Holey carbon coated (SPI, West Chester, PA, USA).

LEO GEMINI SEM (Aachen, Germany) is a high resolution and low voltage SEM equipped with the GEMINI field emission gun. The SEM can be used with acceleration voltages from 0.2 to 30 keV. The GEMINI column provides typical resolutions of 4 nm at 1 keV, up to 1 nm at 30 keV. Samples for SEM analyses were prepared by filtering 2 ml of the pre-concentrated samples over 0.02 μm Anopore inorganic aluminium oxide filters (SPI, Munchen, Germany).

2.3. Stability test

For the stability test, a sample was collected from the Loire river (Orleans) in 5 l bottle. Five hundred milliliters of the sample was fractionated over 0.45 μm filter (Teflon filters, Durapore, Millipore, USA). Filter was rinsed with 250 ml of MQ water and pre-conditioed with 5–10 ml of river water sample (filtrate was discarded) prior filtration. Then, two bottles of 250 ml were filled with the raw sample and other two bottles were filled with the fraction <0.45 μm. 2.5 ml of 1 g l^{-1} NaN_3 solution was added to one bottle of each fraction to obtain a concentration of 10 mg l^{-1} NaN_3 in the sample. The other bottle was kept in its natural state. All fractions were stored at 4 °C in the dark, and were only taken out without any agitation for size analysis. An aliquot (4 ml) of each sample fraction was used to measure the average particle size after different times using photon correlation spectrometry (PCS).

2.4. Sample pre-concentration and loop/injection volumes

Prior to pre-concentration step, samples were sonicated for 10 min to break aggregates induced during the storage time. An aliquot (500 ml) of each sample was concentrated in a polycarbonate cell (Amicon 8400, Millipore, Billerica, MA, USA) equipped with a magnetic stirring bar located shortly above the filter to prevent its clogging during the filtration and to minimize surface coagulation during filtration process by decreasing the thickness of diffusion layer above the membrane [29]. Its major advantage over the more frequently used tangential filtration in hydrochemistry is the very small size of the filter and the low amount of pore space, which minimizes the adsorption inside the filter during filtration. Argon pressure (3 bars) was provided by a portable bottle. Filtration was performed with 1 kD membrane (Amicon, regenerated cellulose, 44.5 mm diameter).

Prior to filtration, the system was cleaned by flushing MilliQ water and 30–50 ml of MilliQ water were filtered and discarded to clean the system. Each filter was washed in MQ water before the experiment and used only once. This greatly decreased the risk of cross-contamination during sample filtration, providing unique conditions of filtration for all samples and allowing high recovery of colloidal particles. Twenty-five-folds pre-concentration was achieved by reducing the sample volume into 20 ml. The concentrated samples were then collected in a Teflon vials and filters were cut into small pieces and immerged in the concentrated solution. Then samples were sonicated for 15 min to re-suspend any particles stuck to the membrane.

In case of SFlFFF, the effect of the injection volume (loop size) on the separation efficiency was investigated using synthetic standard of known size (73 nm) (Nanosphere^{TM} from Duke Scientific Corp., USA). The standard was injected into the SFlFFF with different injection (sample) volumes. The same quantity of particles (2 μg) was injected to the SFlFFF channel with loop sizes of 20, 40, 100, and 250 μl. Thus, particles concentrations were: 100 ppm for the 20 μl loop, 40 ppm for 50 μl loop, and 20 ppm for 100 μl loop and 8 ppm for 250 μl loop. Additionally, the injection volume (loop size) effect was tested on extracted soil colloids. Two different injection volumes of 100 μl and 250 μm at two different concentrations were tested, i.e. the sample injected in to the 250 μl loop size was 2.5-folds diluted relative to the sample injected into the 100 μl loop sample.

3. Results and discussions

3.1. Stability

Fig. 2a and b respectively shows the average particle size measured by photon correlation spectroscopy of the raw samples and of the fraction <0.45 μm with and without the addition of NaN_3. In raw samples, particles size tends to increase with time in both cases (with or without adding NaN_3). Additionally, the size increase is more important without NaN_3 addition. This is presumably due to the presence of high amount of bacteria and large particles, which enhance the probability of aggregation [12]. In the fractionated samples (<0.45 μm), the average particle size shows very low variations with time in both cases (with or without adding NaN_3) thanks to the removal of larger particles and bacteria by filtration over 0.45 μm.

Thus, in order to minimize samples perturbations all samples were filtered over 0.45 μm and a bactericide (NaN_3) was added to samples. The choice of 0.45 μm filtration was due to following reasons: (i) the fraction <0.45 μm is the most important in contaminant transport, (ii) it is a limit below which most of micro organisms (specially bacteria but except viruses) will be removed, (iii) filtered samples are (at least partly) sterilized, and therefore, are less prone to modifications during storage time, (iv) coagulation rate in the fractionated samples (<0.45 μm) may be lower than in raw samples since this process is accelerated by the presence of large particles and bacteria [12], and (v) the fractionation over 0.45 μm allows avoiding the steric/hyperlayer effects. The steric/hyperlayer effects were observed for natural soil colloids of about 500 nm hydrodynamic diameter at comparable cross-flow rates.

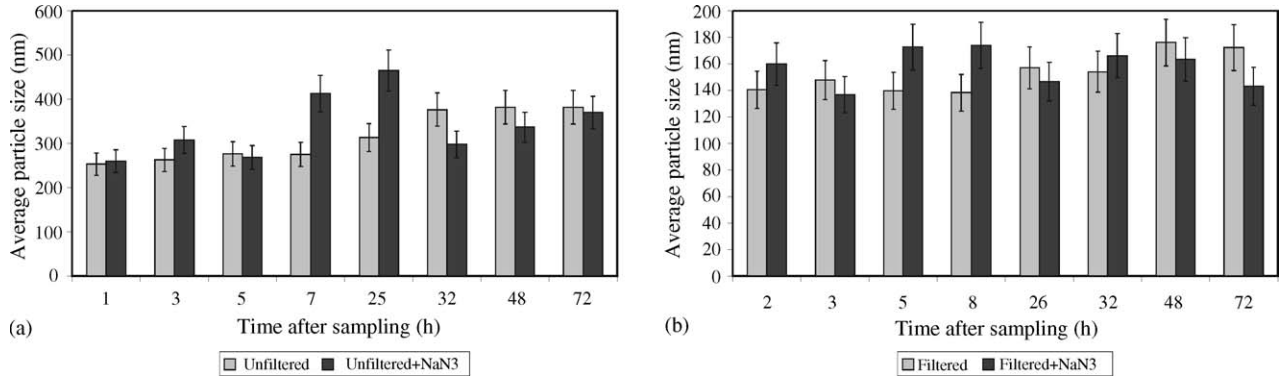

Fig. 2. Variation of particle size over experiment duration in hours (h): (a) unfiltered sample with and without the addition of 2.5 ml of 1 g l^{-1} NaN_3 solution to 250 ml of the sample to obtain a concentration of 10 mg l^{-1} NaN_3 in the sample; (b) same conditions as in (a) but observed in the filtered sample.

3.2. Sample pre-concentration

The low concentration of colloidal particles (1–450 nm) in most natural aquatic systems implies the need to pre-concentrate the samples prior to fractionation by FlFFF in order to obtain adequate signals from the detectors (UV-FLD–MALLS) coupled to FlFFF. In this study, pre-concentration using ultra-filtration stirred cell, larger loop size, on channel concentration, and sensible detectors (FLD and MALLS) are combined to optimize the required concentration step. Nevertheless, artifacts such as aggregation may occur during one or more of these processes. SEM micrographs (Fig. 3) of three samples (Brugeilles, Cezerat and Chatillon) concentrated by the stirred cell (Ultra-filtration) show individually separated colloidal particles less than 450 nm. Thus, these micrographs confirm the gentle pre-concentration step applying the stirred cell. In the following section, potential artifacts due to on-channel concentration and/or artifacts inside the FlFFF channel will be assessed by MALLS and TEM.

The loop size routinely used up to now for SFlFFF in the literature is 20 μl. Fig. 4 shows that, the applied injection loop volume between 20 and 250 μl in SFlFFF to fractionate spherical standard (73 nm) has no effect on its resolution (the peak width is the same). In case of larger loop size, particles elute before than in case of smaller loop size, because the sample is pushed further into the channel by the larger injection volume. Hence, only a smaller part of the channel can be used for fractionation, the effective channel volume decreases correspondingly with increasing loop size. Additionally, Fig. 5 shows also slight variations in the fractograms, and the R_g in case of natural sample. The observed effects of peak shift and distortion are negligible compared to effects arising from 10 to 20-folds external enrichment. Consequently, this result allows reducing the required preconcentration step by 12.5-folds, and therefore, allows to separate low concentrated samples up to separate some natural samples without any pre-concentration (in case of samples with high colloids concentration). Furthermore, this result enhances the amount of particles under analysis, and thus, the amount of particles eluting from the SFlFFF channel. This enhancement will improve the consequent analyses by ICP-MS, TEM, or any other technique.

In case of ASFlFFF, on channel concentration [14] allows the injection of even larger volumes (2 ml), and therefore, reduces further the required external pre-concentration step.

3.3. River samples analysis

Three River samples (Burgeilles, Cezerat and Chatillon) were concentrated and fractionated by SFlFFF and ASFlFFF coupled to (MALLS–UV-FLD–TEM) detectors as described in Section 2. The results are presented in Figs. 6–11. The performance of the FlFFF channel and the usefulness of the data obtained largely depend on the ancillary detectors used after the channel. FlFFF independent detectors contribute significantly to the value of the final data analysis [30]. MALLS, TEM, and FLD are used in this study to draw out the maximum information about samples size distribution. The choice of a detector depends on the nature of the sample, the required information, and the sensitivity of the used detector [30]. In this section, the use of different detectors to investigate FlFFF fractionation behavior and particle size distribution will be discussed in details. Results are presented according to their fractionation behavior inside the FlFFF channel.

3.3.1. Simple (ideal) behavior

Fig. 6a and b shows, respectively, the SFlFFF and ASFlFFF fractograms of a 25-folds concentrated natural colloidal river sample (Burgeilles) using the (250 μl injection volume) for SFlFFF and the (2 ml injection volume) for ASFlFFF. The UV shows no response because the FlFFF eluent concentration is lower than the detection limit of the UV detector. The FLD and the 90° light scattering responses show a hydrodynamic radii distribution in the range 15–250 nm in accordance with the pre-filtration (<0.45 μm) in both cases. Both SFlFFF and ASFlFFF systems show an ideal elution behavior (small particles elute before larger particles and no retardation, or steric elution is observed).

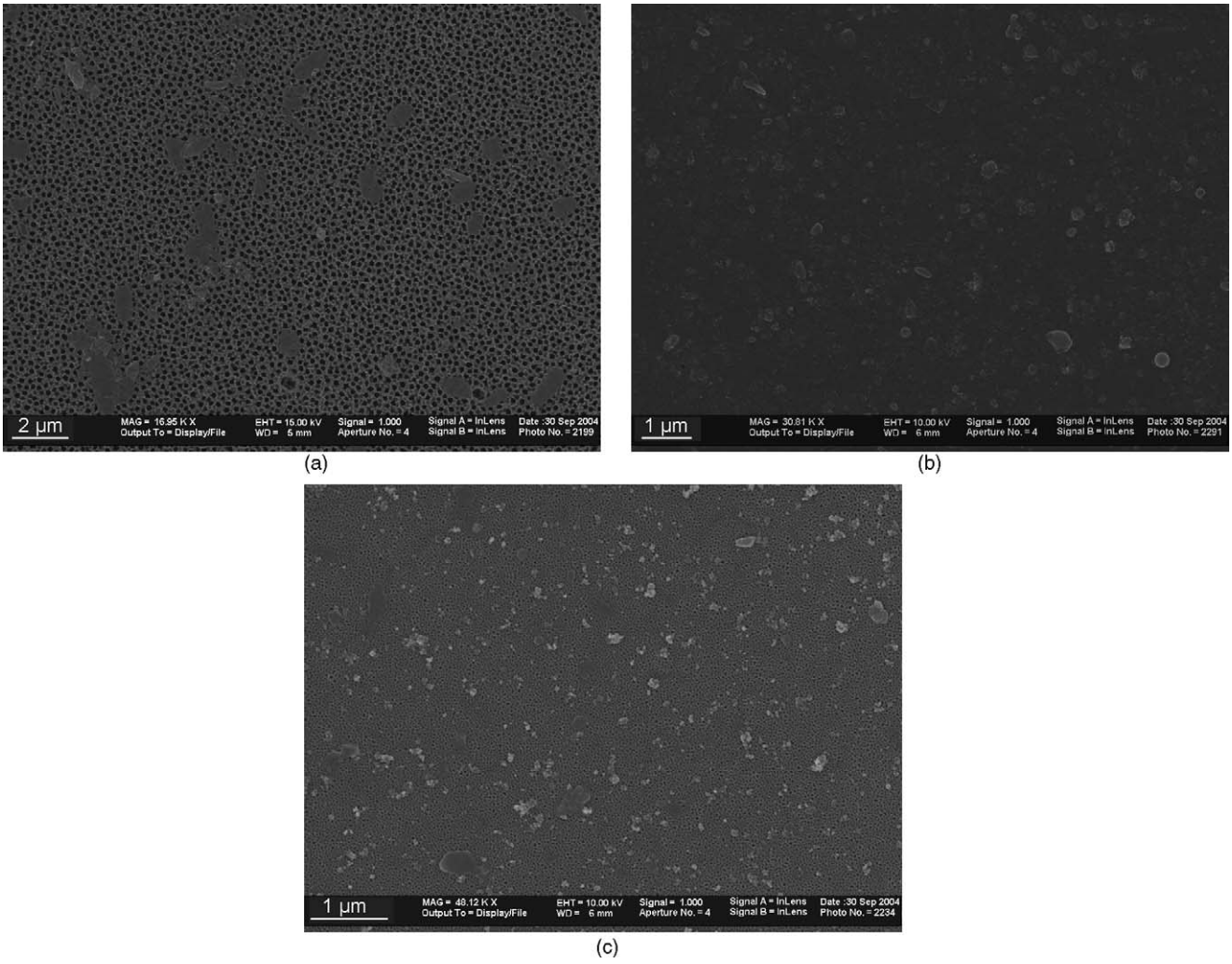

Fig. 3. SEM images of river samples after 25-folds concentration (a) Burgeilles, (b) Cezerat and (c) Chatillons.

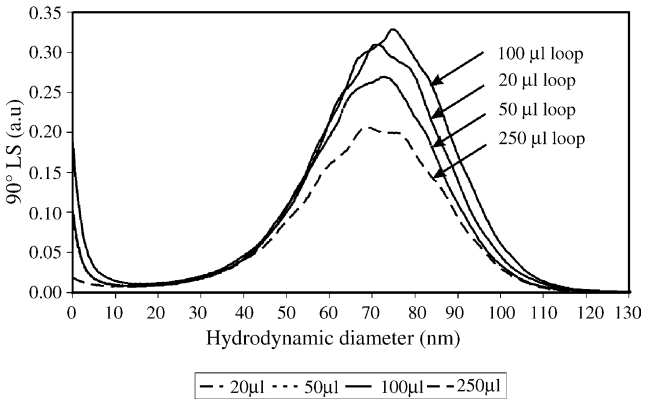

Fig. 4. Loop size effect on the FFF separation using nanospherical particles of 73 nm diameter channel flow 1.0 ml min^{-1}, cross flow 0.5 ml min^{-1}. LS is light scattering, au is arbitrary unit, 20, 50, 100 and 250 µl refer to the loop sizes used.

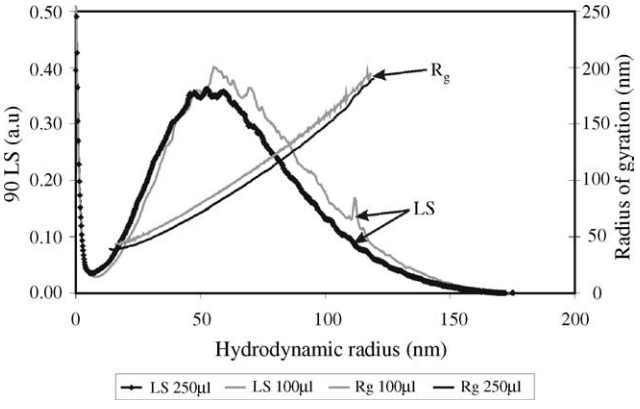

Fig. 5. Loop size effect on the FlFFF fractionation using natural sample, FlFFF conditions are: channel flow 1.0 ml min^{-1}, cross flow 0.3 ml min^{-1}. LS is light scattering, R_g is the radius of gyration, 100, and 250 µl refer to the loop sizes used.

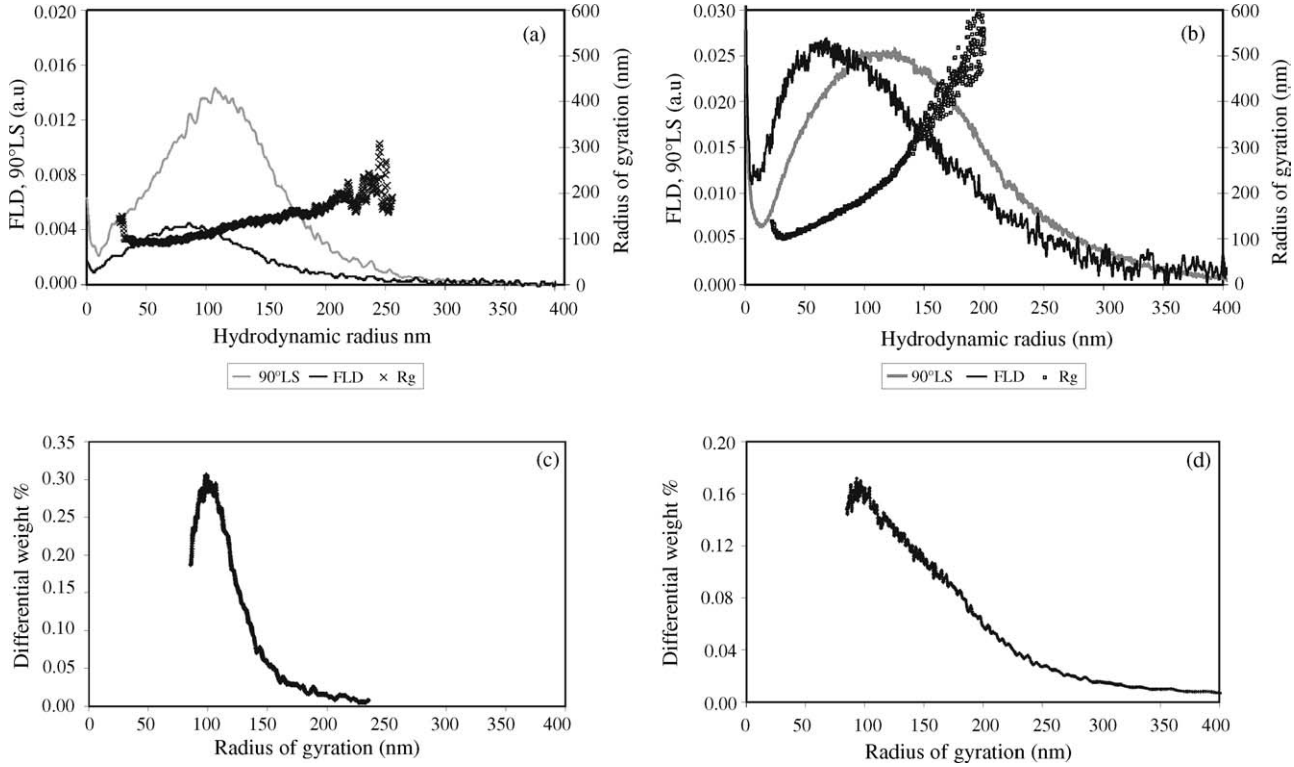

Fig. 6. River sample fractionation by FFF-MALLS–UV-FLD (Burgeilles), (a) SFlFFF with 1.0 ml min^{-1} channel flow and 0.3 ml min^{-1} cross flow (b) ASFlFFF with 1.0 ml min^{-1} channel flow and a gradient cross flow starting at 0.25 ml min^{-1} and decreasing linearly to 0.1 ml min^{-1} during 50 min, (c and d) are the differential weight fractions corresponding to (a and b).

The R_g shows elevated values near the void peak (Fig. 6a and b). These high values are presumably related to the elution of some large particles within the void peak. This behavior is well known and was previously described by Contado et al. [11]. Additionally, the increase of the R_g with the elution volume (and corresponding increase of R_h) confirms the FlFFF fractionation order. However, in case of ASFlFFF, R_g increases faster (for $R_h > 150$ nm) than in case of SFlFFF. This may be related to following reasons: (i) due to the field gradient applied in ASFlFFF, sample slices corresponding to $R_h > 150$ nm are less well fractionated, and thus, may contain a broader mixture of sizes, which will increase the value of R_g calculated for each slice; (ii) the beginning of steric effects (pre-elution of larger particles), which also increases the R_g value compared to R_h; and (iii) artifacts resulting from the removal of big particles and aggregates previously stuck to the FlFFF membrane in case of old FlFFF membrane. From the data presented, it is still not possible to point out the responsible mechanism. However, MALLS allows the assessment of such behaviour as MALLS is an FlFFF independent size measuring detector.

The percentage differential weight fraction for R_g distribution for SFlFFF and ASFlFFF is respectively shown in Fig. 6c and d. The ASFlFFF shows a broader distribution of R_g and a maximum slightly shifted to smaller size. This wider distribution in case of ASFlFFF is related to the detection of larger particles as described above.

TEM fractograms of four fractions collected after SFlFFF fractionation are shown in Fig. 7. These micrographs show certain polydispersity in particles size, which may be related to particles shape variations and to the broadening effects occurring in SFlFFF channel. Particles sizes measured by TEM do not match well with SFlFFF hydrodynamic diameter, or with the MALLS R_g because each of these measures are based on different size properties and uses different principles to measure particles size. FlFFF measures the diffusion coefficient and derives the hydrodynamic radius; MALLS determines radius of gyration, which already incorporates structural and shape information; TEM determines particles cross-section depending on how the particle is placed on the TEM-probe. Nevertheless, these TEM results confirm the increase of particle size with the elution volume, and thus, validate the SFlFFF fractionation order. Furthermore, these micrographs also show some large particles eluting at larger elution volumes (F3 and F4). These large particles signify some artifacts, which may bay related to the same reasons described above for the increase of R_g for $R_h > 150$ nm.

3.3.2. *Complex (non-ideal) behavior*

Figs. 8–11 show the results obtained for two other samples (Cezerat and Chatillon) applying the same methodology. The same result was observed with the UV detector, but only Cezerat sample shows a UV peak shifted toward smaller sizes. The FLD and MALLS 90° light scattering responses

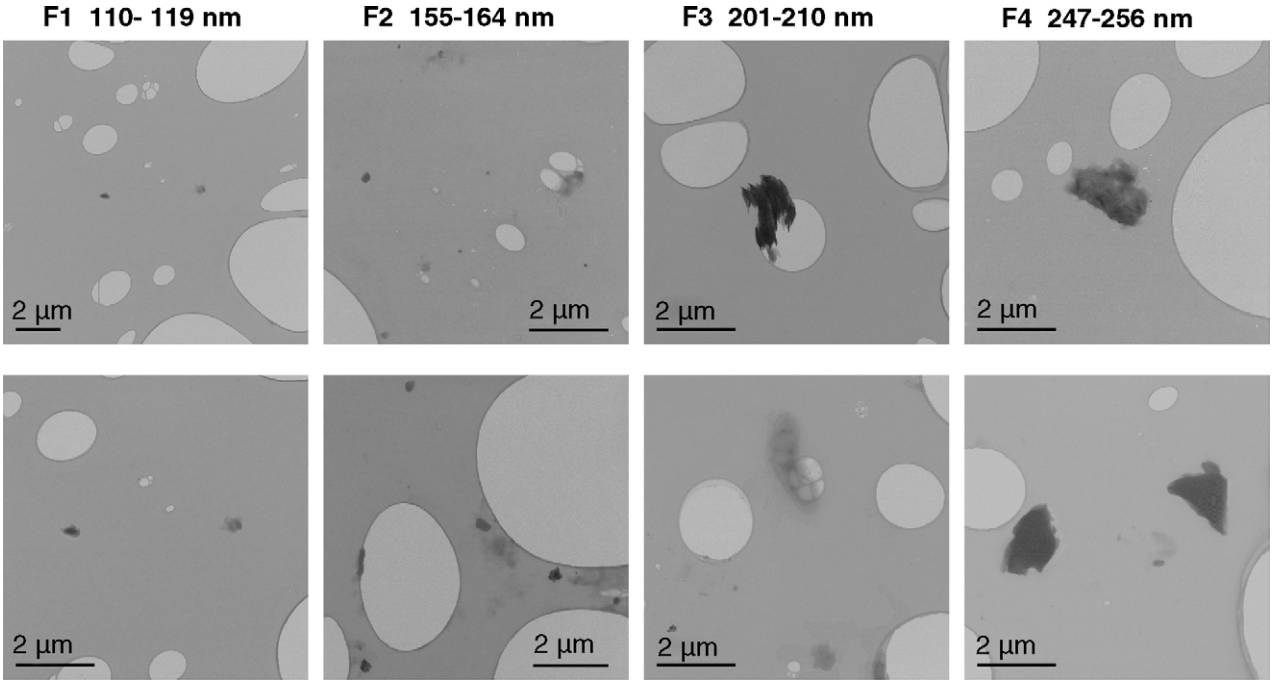

Fig. 7. TEM micrographics of colloidal fractions collected after FFF fractionation of 25-folds concentrated colloidal sample from Burgeilles, France. TEM samples were prepared by deposition of a drop of water on a 300 mesh copper TEM grid covered by a holey carbon membrane.

(Figs. 8 and 10a and b) show a hydrodynamic radius distribution in the range 15–400 nm, signifying a wider size distribution in comparison to Brugeilles sample and consequently, more tailing. The SFLFFF responses show a double peak for Cezerat and a single peak for Chatillon sample; while ASFlFFF shows double peak in both cases. This double peak may signify bimodal colloidal size distribution, or a pre-elution of larger colloidal particles in the ASFlFFF channel due to steric effects. Thus, in this case, the theoretical FlFFF calculation and the calibration with spherical standards cannot explain this behavior. However, only FlFFF independent detectors (MALLS and TEM) can elucidate it.

The same behavior of R_g, as previously described for Brugeilles, was observed near the void peak due to the same reasons. The R_g increases with the elution volume (and thus with R_h) confirming the fractionation order by FlFFF. However, a non-ideal FlFFF fractionation behavior is observed in Figs. 8 and 10. The non-ideal fractionation behavior in Figs. 8a and 10a and b, is manifested in a rapid R_g increase for R_h values superior to 150 nm. While, the non-ideal behavior in Fig. 8b, is a little bit different: R_g increases with R_h according to FlFFF theory in the range of $R_h < 80$ nm, then R_g shows a constant value with R_h in the range of R_h (80–150 nm), and after that, the R_g increases more rapidly than the R_h in the range of $R_h > 150$ nm. This behavior is not observed with SFlFFF (Fig. 8a). The constant R_g values in the range of R_h (80–150 nm) may be related to particles-membrane interaction, and hence, delay in elution of particles of comparable sizes. The rapid increase of R_g for colloids with $R_h > 150$ nm, may be related to a pre-elution of large colloidal particles due

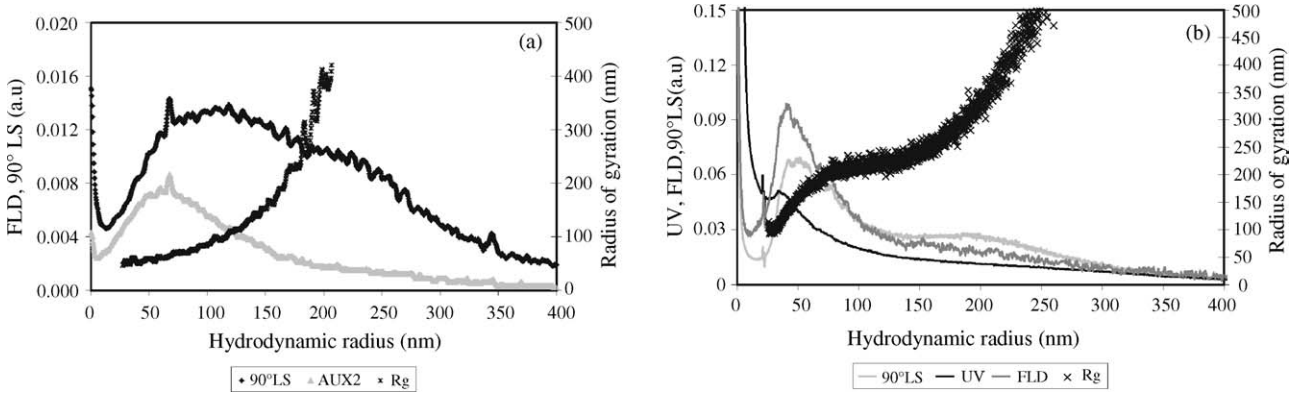

Fig. 8. River sample fractionation by FFF-MALLS–UV-FLD (Cezerat), (a) SFlFFF with 1.0 ml min^{-1} channel flow and 0.3 ml min^{-1} cross flow and (b) ASFlFFF with 1.0 ml min^{-1} channel flow and a gradient cross flow starting at 0.25 ml min^{-1} and decreasing linearly to 0.1 ml min^{-1} during 50 min.

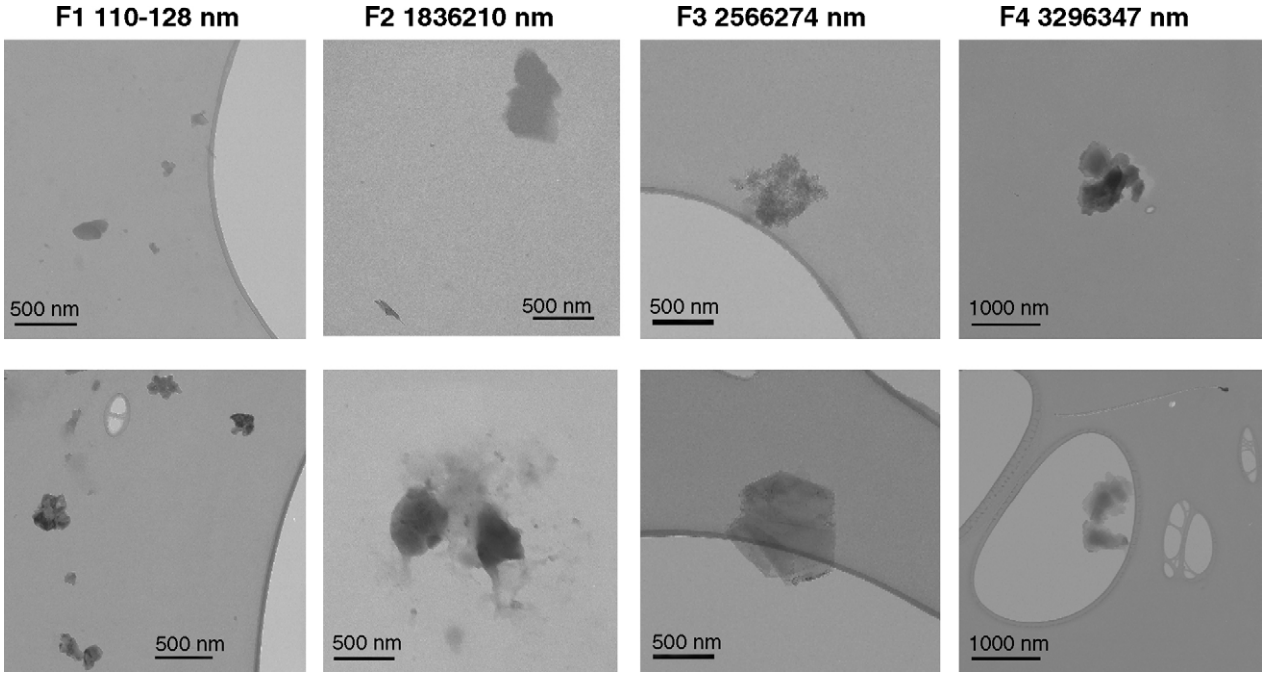

Fig. 9. TEM micrographics of colloidal fractions collected after FFF fractionation of 25-folds concentrated colloidal sample from Cezerat, France. TEM samples were prepared by deposition of a drop of water on a 300 mesh copper TEM grid covered by a holey carbon membrane.

to steric effects, or to an insufficient fractionation due to cross flow reduction. Consequently, in this case, FlFFF fractionation theory is valid for the size range of R_h (15–150 nm), but not any more valid for larger particles. For that reason, no percentage differential weight calculation were carried out for these samples.

TEM micrographs of fractions collected (after SFlFFF fractionation) are shown in Figs. 9 and 11, respectively, for Cezerat and Chatillons. These micrographs show certain poly-dispersity in particles size due to particles shape variations and to the broadening effects through the SFlFFF channel as shown previously for Brugeilles. Particles sizes measured by TEM do not match well with the results obtained by SFlFFF (R_h) and by MALLS (R_g). These deviations between TEM, FlFFF, and MALLS results are due to fact that each of these technique measure different aspects of particle size based on different principles. Nevertheless, TEM micrographs (Figs. 9 and 11) in addition to MALLS measurements (Figs. 8 and 10) illustrate particles size increase with elution volume, and consequently, confirm FlFFF fractionation order as previously described for Brugeilles sample. The first two fractions (F1 and F2) micrographics show small particles sizes and less polydisperse particles than the two (Fig. 9)/three (Fig. 11) other fractions (F3–F5). F1 and F2 correspond to ideal particles fractionation by the SFlFFF, while the other fractions (F3, F4, and F5) correspond to large particles size distribution. Thus, F3–F5 contain particles eluting under the influence of steric effects and probably large particles interacting with the membrane in SFlFFF channel.

For all samples, FlFFF calibration and MALLS measurements reveal larger particles than the filter pore size (0.45 μm) used for pre-fractionation of the samples. This may be related

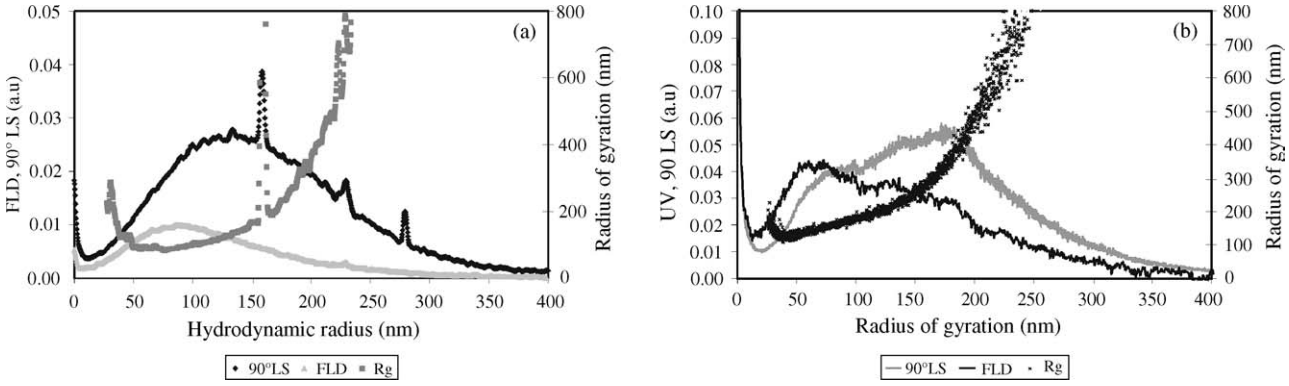

Fig. 10. River sample fractionation by FFF–MALLS–UV-FLD (Chatillons), (a) SFlFFF with 1.0 ml min^{-1} channel flow and 0.3 ml min^{-1} cross flow (b) ASFlFFF with 1.0 ml min^{-1} channel flow and a gradient cross flow starting at 0.25 ml min^{-1} and decreasing linearly to 0.1 ml min^{-1} during 50 min.

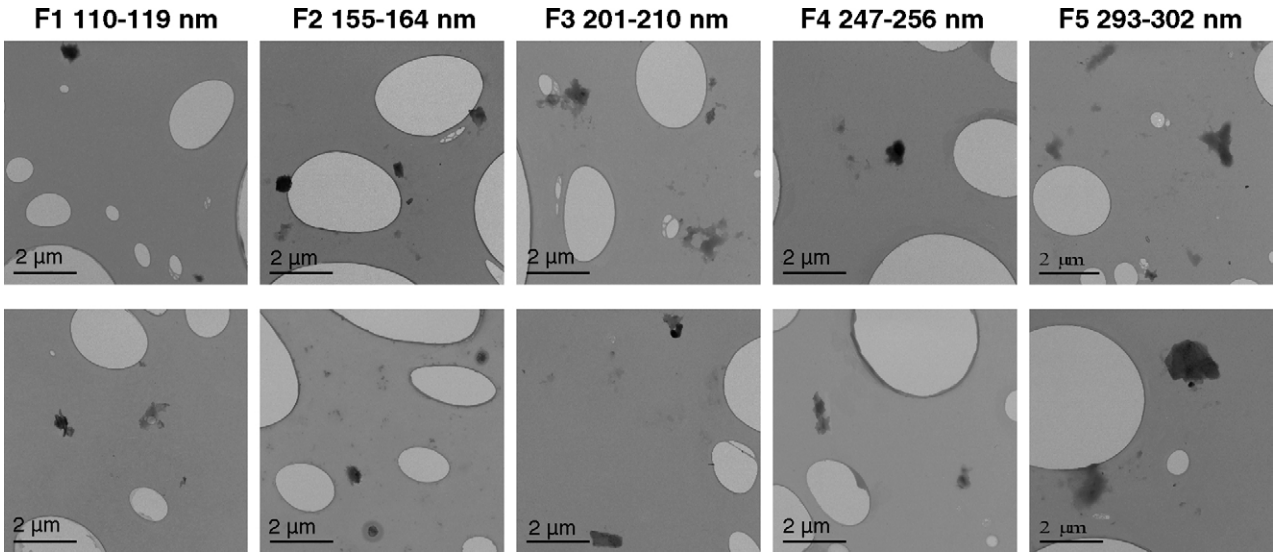

Fig. 11. TEM micrographics of colloidal fractions collected after FFF fractionation of 25-folds concentrated colloidal sample from Chatillons, France. TEM samples were prepared by deposition of a drop of water on a 300 mesh copper TEM grid covered by a holey carbon membrane.

to the following reasons: (i) the given filter pore size is a nominal size through which some larger particles can pass, (ii) natural samples are never spherical, some elongated particles can go through the filter, which may have larger equivalent hydrodynamic radius or radius of gyration, (iii) some large single particles may occur as artifacts such as particles released from the FlFFF membrane in case of old membranes, and (iv) some large particles can be generated in the channel during focussing or relaxation due to aggregation.

To sum up, these results show that: using larger injection loop size, sample pre-concentration, using more sensitive and FlFFF independent detectors (FLD, MALLS, and TEM); it is possible to fractionate, and characterize very low concentrated colloidal river samples. Results also confirm that, FlFFF independent detectors can be used to control colloids fractionation behavior inside the FlFFF channel (normal fractionation, steric behavior, aggregation, retardation, etc.).

The 0.45 μm cutoff was useful to avoid the co-elution of small colloidal particles with those larger than the critical steric inversion diameter. The inversion of the elution order may generate fractions containing particles with two different diameters, and consequently, incorrect size distribution. This misleading in particle size fractionation could not be detected by the UV alone. The use of another type of detectors measuring the absolute particle size is essential in order to detect this co-elution behavior. MALLS and TEM are the techniques of choice as they determine the absolute particle size independently of the FlFFF.

4. Conclusion

This work presents a refined methodology for sample collection, preservation, stabilization, size fractionation, and characterization for natural (river) colloids by FlFFF–MALLS–TEM. MALLS and TEM determines colloidal size independently from FlFFF elution conditions. Consequently, these two techniques allow more reliable determination of colloidal size than calibration by spherical standards.

Furthermore, this study demonstrates the usefulness of MALLS and TEM as control techniques of the FlFFF fractionation performance. MALLS resolved an ideal behavior in the case of Brugeilles sample and a potential transition to steric/hyperlayer elution mode for larger colloids ($R_h > 150$ nm) in Cézerat and Chatillon samples. Additionally, FLD and MALLS illustrated that, SFlFFF and ASFlFFF show slight differences in particle size distribution for the same sample. A major disadvantage of TEM is the tedious nature of the measurements and the long time required for analysis. Therefore, MALLS can be used as an alternative and routine technique to control the FlFFF elution behavior of colloids. The use of several techniques in parallel after FlFFF acts as cross check on the possible artifacts and makes FlFFF a more reliable technique.

These results recommend FlFFF–UV-FLD–MALLS–TEM couple as a technique of choice for colloids fractionation and size determination. They suggest that, FlFFF will have further applications in understanding the environmental role of colloids. One of our previous studies showed the utility of FlFFF–MALLS–TEM to study colloids sedimentation. Another study (under preparation) coupling the FlFFF to the ICP-MS illustrates the usefulness of this technique in studying the interaction between trace elements and colloids (organic and inorganic).

References

[1] L. Denaix, R.M. Semlali, F. Douay, Environ. Pol. 114 (2001) 29.
[2] Y. Ran, J.M. Fu, G.Y. Sheng, R. Beckett, B.T. Hart, Chemosphere 41 (2000) 33.

[3] J.F. McCarthy, Phys. Chem. Earth 23 (1998) 171.
[4] M.B. McGechan, Biosys. Eng. 83 (2002) 387.
[5] M.B. McGechan, D.R. Lewis, Biosys. Eng. 83 (2002) 255.
[6] A.L. Noell, J.L. Thompson, M.Y. Corapcioglu, I.R. Triay, J. Chromatogr. A 31 (1998) 23.
[7] M.L. Wells, G.J. Smith, K.W. Bruland, Marine Chem. 71 (2000) 143.
[8] M.L. Wells, P.B. Kozelka, K.W. Bruland, Marine Chem. 62 (1998) 203.
[9] R. Beckett, Z. Jue, C. Giddings, Environ. Sci. Technol. 21 (1987) 289.
[10] R. Beckett, D.M. Hotchin, B.T. Hart, J. Chromatogr. 517 (1990) 435.
[11] C. Contado, G. Blo, F. Fagioli, F. Dondi, R. Beckett, Colloids Surf. A: Physicochem. Eng. Aspects 120 (1997) 47.
[12] J. Buffle, H. Leeuwen (Eds.), Environmental Particles I, CRC press, Boca Raton, FL, 1992.
[13] J. Buffle, H.P.V. Leeuwen (Eds.), Environmental Particles II, CRC press, Boca Raton, FL, 1993.
[14] J. Ranville, R. Beckett, in: M.E. Schimpf, K. Caldwell, J.C. Giddings (Eds.), Field Flow Fractionation Handbook, Wiley, New York, 2000, p. 507.
[15] M. Hassellöv, B. Lyvén, R. Beckett, Environ. Sci. Technol. 33 (1999) 4528.
[16] R. Beckett, G. Nicholson, B.T. Hart, M. Hansen, J.C. Giddings, Water Res. 22 (1988) 1535.
[17] L.J. Gimbert, K.N. Andrew, P.M. Haygarth, P.J. Worsfold, Trends Anal. Chem. 22 (2003) 615.
[18] M.E. Schimpf, M.P. Petteys, Colloids Surf. A: Physicochem. Eng. Aspects 120 (1997) 87.
[19] G. Yohannes, S.K. Wiedmer, M. Jussila, M.-L. Riekkola, Chromatography 61 (2005) 359.
[20] J.C. Giddings, in: M.E. Schimpf, K. Caldwell, J.C. Giddings (Eds.), Field Flow Fractionation Handbook, Wiley, New York, 2000, p. 3.
[21] F. v.d.Kammer, M. Baborowski, K. Friese, Anal. Chim. Acta, 2005 (accepted with revisions).
[22] P.J. Wyatt, J. Colloid Interface Sci. 197 (1998) 9.
[23] P.J. Wyatt, Anal. Chim. Acta 272 (1993) 1.
[24] R. Beckett, D. Murphy, S. Tadjiki, D.J. Chittleborough, J.C. Giddings, Colloids Surf. A: Physicochem. Eng. Aspects 120 (1997) 17.
[25] M. Baalousha, F.v.d. Kammer, M. Motelica-Heino, H.S. Hilal, P. Le Coustumer, J. Chromatogr., 2005 (accepted with revisions).
[26] M. Baalousha, M. Motelica-Heino, N. Guigues, F. Huneau, G. Braibant, P. Le Chem. Geol., submitted for publication.
[27] V.M. Gun'ko, A.V. Klyueva, Y.N. Levchuk, R. Lebodac, Adv. Colloid. Interface 105 (2003) 201.
[28] J.P. Pinheiro, A.M. Mota, J.M.R. d'Oliveira, J.M.G. Martinho, Anal. Chim. Acta 329 (1996) 24.
[29] J. Buffle, G.G. Leppard, Environ. Sci. Technol. 29 (1995) 2176.
[30] M.N. Myers, L.E. Oppenheimer, M.E. Schimpf, in: M.E. Schimpf, K. Caldwell, J.C. Giddings (Eds.), Field Flow Fractionation Handbook, Wiley, New York, 2000, p. 213.